



Investigating the performance of a greenhouse gas observatory in Hefei, China

Wei Wang¹, Cheng Liu^{2,1*}, Wenqing Liu¹, Pinhua Xie¹, Jianguo Liu¹, Youwen Sun¹,
Yuan Tian¹, Jin Xu¹, Isamu Morino³, Voltaire A. Velazco⁴, David. W. T. Griffith⁴

¹Key Laboratory of Environmental Optics and Technology, Anhui Institute of Optics
and Fine Mechanics, Chinese Academy of Sciences, Hefei, 230031, China

²University of Science and Technology of China, Hefei, 230026, China

³Satellite Observation Center, National Institute for Environmental Studies, Japan

⁴School of Chemistry, University of Wollongong, Northfields Ave, Wollongong,
NSW, 2522, Australia

Correspondence to: Cheng Liu (chliu81@ustc.edu.cn)

Abstract: A ground-based high resolution Fourier Transform Spectrometer (FTS) station has been established in Hefei, China to remotely measure CO₂, CO and other trace gases based on near-infrared solar absorption spectra. Total columns of atmospheric CO₂ and CO have been successfully measured from July 2014 to April 2016. Daily and monthly average column-averaged dry air mole fraction of CO₂ showed a clear seasonal cycle, while the daily and monthly average of XCO displayed no seasonal variation. The spectra collected with an InSb detector in the first year were compared with those collected by an InGaAs detector from July 2015, demonstrating that InGaAs spectra have better signal-to-noise ratios and RMS spectral fitting residuals relative to InSb spectra. Consequently, the measurement precision of the retrieved XCO₂ and XCO for InGaAs spectra is superior to InSb spectra, with about 0.04 % and 0.09 % for XCO₂, 1.07 % and 2.00 % for XCO within clear sky days, respectively. We analyzed the relationship of daily average XCO₂ and XCO on seasonal scale, found that although there was very weak correlation between them in summer and fall, there existed strong correlation in winter and spring. The CO₂/CO correlation slope was 126.62 and 94.32 ppm/ppm in winter and spring for 2014-2015 and 2015-2016, respectively. The direct comparison of our observations with GOSAT data shows good agreement of daily average and monthly average XCO₂, with biases of -0.64 ppm and -0.49 ppm, and standard deviations of 1.27 ppm and 1.12 ppm, respectively. The correlation coefficient (R^2) is 0.87 and 0.92 for daily and monthly average XCO₂ between our FTS and GOSAT observations, respectively. Daily average OCO-2 data produce a positive bias of 1.00 ppm and standard deviation of 1.92 ppm relative to our ground-based data, and the monthly average OCO-2 data give a bias of 1.07 ppm and standard deviation of 1.62 ppm. Our daily and monthly average XCO₂ also show strong correlation with OCO-2 data, with correlation coefficient (R^2) of 0.81 and 0.85, respectively. Although there were a limited number of data during the observations due to instrument failure and adverse weather, the results confirm the suitability of the observatory for long term measurements of



30 greenhouse gases with high precision and accuracy.

Keywords: Total column, Carbon dioxide, Carbon monoxide, Satellite data, Fourier Transform Spectrometer.

1. Introduction

35 Global warming is an important issue facing humankind, and is largely due to anthropogenic emissions of greenhouse gases. The most important anthropogenic greenhouse gas, carbon dioxide continues to increase at a rate of approximately 2.0 ± 0.1 ppm/year for 2002-2011 despite emission reduction efforts worldwide (IPCC 2014). The primary sources of the increased atmospheric carbon dioxide are fossil
40 fuel combustion and land-use change due to deforestation. At the present time, the two anthropogenic sources release more than 9 GtC/year into the atmosphere (IPCC 2014; Le Quéré et al., 2014). However the knowledge of CO₂ source and sink distributions is still uncertain. In order to predict future climate change and understand the carbon cycle, more measurements are needed to improve understanding of the CO₂ sources
45 and sinks.

Atmospheric CO, an indirect greenhouse gas, is an ozone precursor and a major pollutant in the troposphere. The main sources for CO in the atmosphere are biomass burning, fossil fuel combustion and oxidation of methane and nonmethane hydrocarbons (Clerbaux et al., 2008; Yin et al., 2015). The main sinks of CO in the
50 troposphere are oxidation reaction with the hydroxyl radical (OH). CO plays an important role in atmospheric chemistry because it has an important effect on the oxidizing capacity of the troposphere.

Many techniques and methods have been successfully utilized in surface in situ measurement of atmospheric CO₂, CO, CH₄, and N₂O (Newman et al., 2013; Sarangi et al., 2014; Vardag et al., 2014; WMO 2014; Buchholz et al., 2015; Schibig et al.,
55 2015). Although these in situ measurements made at surface sites show high accuracy and precision, their usefulness in determining the global strengths and distributions of source and sink for greenhouse gases is limited due to their sparse spatial coverage. One way to improve the spatial and temporal sampling of CO₂ and other trace gases is
60 to obtain column abundances from space-based instruments, for example, SCIAMACHY onboard ENVISAT, TANSO-FTS onboard GOSAT and grating spectrometers onboard OCO-2 (Bovensmann et al., 1999; Bovensmann et al., 2004; Crisp et al., 2004; Hamazaki et al., 2005; Kuze et al., 2009; Boesch et al., 2011; Frankenberg et al., 2015). The data derived from space have provided useful
65 information to constrain the carbon cycle, but still need to be validated and improved in sensitivity and resolution.

Ground-based high resolution Fourier transform spectrometers can accurately and precisely measure total columns of CO₂, CO, CH₄, N₂O and other gases (Yurganov et al., 2005; Washenfelder et al., 2006; Deutscher et al., 2010; Wunch et al., 2011a; Dohe,
70 2013; Rokotyan et al., 2014; Wang et al., 2014). The Total Carbon Column Observing Network (TCCON) is a network of ground-based FTS dedicated to simultaneous



retrieval of column-averaged abundances of atmospheric constituents, by recording direct solar spectra in the near infrared region. In order to provide insights into the carbon cycle, the CO₂ total column data resulting from the TCCON sites require a precision of better than 0.1 % (Olsen and Randerson, 2004). It has been demonstrated that TCCON measurement can achieve high accuracy and precision, for example, the claimed accuracy of column averaged dry air mole fraction of CO₂ is better than 1 % and precision is higher than 0.25 % (1 ppm for CO₂) (Deutscher et al., 2010; Wunch et al., 2010; Messerschmidt et al., 2011). In addition, the data from TCCON stations have been used to calibrate and validate measurements from satellite, and also play a role for validation of atmospheric modeling studies (Morino et al., 2011; Reuter, et al., 2011; Schneising, et al., 2012; Guerlet et al., 2013; Dils et al., 2014; Lindqvist et al., 2015; Ohyama et al., 2015; Kulawik et al., 2016). However, the present limitation of the TCCON measurements is the sparseness of their spatial coverage for carbon cycle research and validation of satellites, especially in the Asian region. So far no publications involved in TCCON measurement have been reported in China. In this paper a high resolution FTS dedicated to near continuous observation of solar spectra deployed at Hefei in China is described. At present the observation project at the Hefei site may be one of the few operations using high resolution FTS to sample solar spectra in China, so our measurements are very important to provide information for constraining regional sources and sinks. An additional research aim is to validate satellite data, such as GOSAT, in orbit since January 2009, OCO-2, in orbit since July 2014, and TANSAT to be launched in late 2016 by China. In this paper, we investigate the potential of ground-based FTS to accurately and precisely determine temporal variability of atmospheric CO₂ and CO at our measurement site in Hefei, China, and assess the ability of our observations to validate satellite data.

2. Measurement site and instrumentation

The Hefei site (31° 54' N, 117° 10' E, 29 m above sea level), adjacent to a lake in a flat terrain, is located in the northwest rural area of Hefei city in east of China (Fig. 1). It is part of the Anhui Institute of Optics and Fine Mechanics, operated by Key Laboratory of Environmental Optics and Technology, Chinese Academy of Sciences. We installed the instrument consisting of a Bruker IFS 125HR spectrometer and solar tracker in January 2014. Hefei site currently seeks to establish measurements according to TCCON measurement standard, and we are making efforts to become part of TCCON network.

The FT spectrometer (IFS 125HR, BrukerOptics, Germany) has nine scanner compartments, with a maximum resolution of 0.00096 cm⁻¹, as shown in Fig. 2. The solar tracker (STCA83C0, BrukerOptics, Germany) is mounted inside a dome (35 m above sea level) controlled by a motor on the roof of the laboratory building, which directs the solar beam into the spectrometer situated in the laboratory below. Tracking precision of ±0.1° can be achieved with the Camtracker mode. The spectrometer used a liquid nitrogen cooled InSb detector (1,850–1,1000 cm⁻¹) with a CaF₂ beamsplitter to record solar spectra until the end of July 2015. A room-temperature operating InGaAs detector (3,800–1,1000 cm⁻¹) has been used since July 2015. A dichroic



115 mirror will be installed to collect NIR and MIR spectra simultaneously with InSb and
InGaAs detectors with dual acquisition model, and this setup is an extension of the
standard TCCON setup (Kiel et al., 2016a; Kiel et al., 2016b).
Additionally, a weather station (ZENO, Coastal Environmental Systems, USA)
120 monitoring surface pressure, surface temperature, relative humidity, wind speed, wind
direction, solar radiation, rain rate or snow rate, and leaf wetness was mounted near
the solar tracker on the roof in September 2015. At the same time pressure,
temperature and relative humidity indoors are logged via a sensor continuously.

3. Instrumental line shape (ILS) monitoring

Knowledge of the ILS is required to diagnose the alignment of the spectrometer and
125 hence to retrieve total columns of gases from measurements accurately (Hase et al.,
1999; Hase et al., 2013). HCl cell measurements using NIR lamp as source are carried
out regularly from October 2015 when two calibrated HCl cells provided by Caltech
arrived at our site. The ILS retrievals are done using LINEFIT12. The modulation
efficiency (ME) amplitudes and phase errors are shown in Fig. 3. The average loss in
130 ME amplitude at maximum OPD is 1.9 ± 0.8 %, and the phase errors are lower than
0.01. The ILS results show the good alignment and stability of the instrument over the
whole period.

4. Data processing and analysis

A spectral resolution of 0.02 cm^{-1} is employed with the maximum optical path
135 difference of 45 cm to record the interferograms. Two successive scans
(forward-backward) are collected with an acquisition time of approximately 90
seconds. Figure 4 illustrates typical solar spectra collected by the InSb and InGaAs
detectors. The signal-to-noise ratio of typical InSb spectra compared with InGaAs
spectra is summarized in Sect. 5.1.

140 The standard TCCON GFIT retrieval fitting algorithm is used to analyze the spectra
recorded by the FTS. GFIT is a nonlinear least-squares fitting algorithm, developed as
a standard spectral analysis tool for FTS spectra (Wunch et al., 2011a; Wunch et al.,
2015). The atmospheric forward model is used to calculate synthetic transmittance
spectra from molecular absorption coefficients, atmospheric ray paths, a priori
145 profiles for temperature, pressure and water vapor from NCEP/NCAR reanalysis, and
a priori vertical profiles for each trace gas. Then an inverse method compares the
calculated spectra with the measured spectra, and iteratively scales the gas vertical
profiles to minimize the root mean square of fitting residual. The fitting residual is
defined as (Yang et al., 2002; Yang et al., 2005; Rokotyan et al., 2015):

$$150 \quad \chi^2 = \sum_{i=1}^{N_M} \frac{(y_i^M - y_i^C(\alpha, \beta, v_i + \delta, \gamma_1 x_1, \dots, \gamma_n x_n))^2}{\sigma_i^2} \quad (1)$$

where y_i^M is the measured spectrum, y_i^C is the calculated spectrum; v_i is the
frequency in the i th spectral channel, δ is the frequency shift of the measured
spectrum; α and β are the continuum level and tilt; $\gamma_1, \dots, \gamma_n$ are scaling



factors of target gases x_1, \dots, x_n ; n is the number of fitted gases; σ_i is the
155 uncertainty of y_i^M ; N_M is the number of spectral channel.

The column abundance of a gas is obtained by integrating the scaled gas dry air mole
fraction profiles under the best spectral fit. To cancel out some systematic errors, the
derived column abundances of gases are converted to column-averaged dry air mole
fraction (DMF), using the column abundance of O_2 as an internal standard:

$$160 \quad X_{gas} = 0.2095 * \frac{column_{gas}}{column_{O_2}} \quad (2)$$

where $column_{gas}$ and $column_{O_2}$ are the column abundance of gas of interest and O_2 ,
respectively, X_{gas} is the calculated column-averaged DMF.

For processing the data collected before installing the weather station (on Sep 18,
2015), we use meteorological parameters from a weather station about 1km from our
165 laboratory. The spectral windows for retrieval of column CO_2 , CO and O_2 are listed in
Table 1, and are the standard GFIT windows. For CO_2 and CO , the retrieved column
abundances from the two spectral windows were averaged and then converted into
column-averaged DMF. We applied the TCCON calibration factor of 0.989 for XCO_2
(Wunch et al., 2010; Messerschmidt, et al., 2011).

170 5. Results and discussion

5.1 Comparison of InSb and InGaAs spectra

The direct absorption spectra collected under clear sky weather conditions from July
2014 through April 2016 are analyzed here. Spectra from July 2014 to July 2015 were
175 collected with the InSb detector, while the spectra were collected by the InGaAs
detector from July 2015 to April 2016. Spectra with solar intensity variation during
the scan more than 5 % are removed.

The signal-to-noise ratio of a typical InGaAs spectrum compared with an InSb
spectrum is summarized in Table 2. Signal-to-noise ratios of InGaAs spectra are 2-4
times higher than those of InSb spectra in the near infrared region.

180 It is also important to assess the spectral fitting. Figure 5 through 9 depict typical
spectral fitting for InSb and InGaAs spectra. The measured spectra are shown in black,
the fitted spectra in red and the residual in dark cyan. Figure 5 compares typical
spectral fitting of CO_2 in the spectral window centered at 6220 cm^{-1} . The RMS
spectral fitting residuals are about 0.32 % and 0.19 % for InSb and InGaAs spectra,
185 respectively. Figure 6 is a plot of typical spectral fitting of CO_2 in the window
centered at 6335 cm^{-1} , showing the RMS fitting residuals of 0.31 % and 0.21 % for
InSb and InGaAs spectra, respectively. Figure 7 plots typical spectral fitting of CO
in one spectral window centered at 4233 cm^{-1} using two detectors. The RMS spectral
fitting residuals are about 0.52 % and 0.50 % for InSb and InGaAs spectra,



190 respectively. Figure 8 compares typical spectral fitting of CO in the other window
centered at 4290 cm^{-1} , with the RMS error of fitting residuals about 0.54 % and
0.46 %, respectively. Also, typical spectral fitting of O₂ in spectral regions between
7765 cm^{-1} and 8005 cm^{-1} give 0.37 % and 0.29 % RMS for fitting residual, as plotted
in Fig. 9. We conclude that all the RMS error of fitting residuals of InGaAs spectra are
195 small relative to those of InSb spectra, as listed in Table 2.

Further, the measurement precision (repeatability) of the total columns are compared.
The standard deviation of the retrieved column-averaged DMF from spectra sampled
in one hour around noon in a clear sky day (cloud free) is calculated as a measure of
precision. The data of 24 October 2014 and 4 August 2015 are used to infer
200 measurement precision. The measurement precisions of X_{gas} for typical InGaAs
spectra compared to InSb spectra are listed in Table 3. For both CO₂ and CO, the
InGaAs precision is about two times better than the InSb precision.

Recent TCCON measurements have shown that the precision of the resulting mole
fractions is about 0.15 % for CO₂ and 0.5 % for CO (Toon et al., 2009; Messerschmidt
205 et al., 2010; Wunch et al., 2010). So our retrieval results for CO₂ is comparable to
other TCCON stations, whereas the results of CO show poorer precision. From the
comparison of SNR, RMS error of fitting residuals and measurement precision for
InGaAs and InSb spectra, it is preferable to use the InGaAs detector to collect the near
infrared solar spectra rather than InSb detector.

210 **5.2 Variation in column value of CO₂ and CO**

Time series of total column amounts of CO₂ and CO from July 2014 to April 2016 are
presented in Fig. 10. The data are not continuous with gaps due to scanner failure or
adverse weather conditions, especially in February and March 2015. The CO₂ column
varied from 8.18×10^{21} to 9.05×10^{21} molecules cm^{-2} throughout the period, while
215 column CO was in the range between 1.73×10^{18} and 4.07×10^{18} molecules cm^{-2} . It is
noted that column O₂ lies between 4.39×10^{24} and 4.75×10^{24} molecules cm^{-2} , with
mean value and standard deviation of 4.59×10^{24} and 5.26×10^{22} molecules cm^{-2} ,
respectively. The scatter for column O₂ is about 1.15 % (Fig. 11). Over this time
period, the atmospheric pressure spanned from 1001.3 to 1043.5 hPa, and the mean
220 value and standard deviation were 1021.0 and 8.02 hPa, respectively, corresponding to
scatter of 0.79 %, which is comparable to the variation of column O₂.

Figure 12 is time series of X_{air} (defined as the column-averaged abundance of dry air),
with the value in the range between 0.96 and 1.02. The mean value is 0.98, with the
standard deviation of 0.005 (0.49 %), consistent with other TCCON sites. The low
225 scatter in time series of X_{air} means that the stability of our measurements is high.

5.3 Daily, monthly and annual variability of XCO₂ and XCO

Time series of individual measurements, daily averages and monthly averages of
column-averaged DMF of CO₂ are plotted in Fig. 13. The sampling days with the
number of data points less than 10 are not considered due to lack of representativeness.
230 Figure 13 suggests that variation of XCO₂ showed clear seasonal cycle, XCO₂ reached
the minimum in late summer, then slowly increased to the highest value in spring. The



daily average XCO₂ ranged from 392.33 to 411.62 ppm, and the monthly average value showed that the seasonal amplitude was 8.31 and 13.56 ppm for 2014 through 2015 and for 2015 through 2016, respectively. Biosphere-atmosphere exchange has the most effect on the atmospheric constituents at such low altitude locations as Hefei site. August and September are still growth season with higher temperature, and photosynthesis playing a dominant role as CO₂ sink in this period, resulting in the minimum CO₂ in late summer. Photosynthesis gradually ceases and respiration becomes a major source from October, so CO₂ builds up in winter and spring. Our observations may also be affected by regional anthropogenic emissions because the site is about 10 km northwest of the Hefei urban area (population 7.7 million), so the variability pattern of CO₂ resulted from the combined effects of photosynthesis, respiration and anthropogenic emissions.

In the recent study of Wunch et al. (2011b), the ACOS-GOSAT data and FTS observation in 2009-2010 indicated that XCO₂ in the Japanese Tsukuba station had clear seasonal cycle, with a maximum in winter and a minimum in summer. In Butz et al. (2011), the observations from GOSAT and the co-located ground-based measurements captured the seasonal cycle of XCO₂ with the late summer minimum and the spring maximum for four TCCON stations in the northern hemisphere. In Schneising et al. (2014), XCO₂ determined by SCIAMACHY and CarbonTracker for the Northern Hemisphere (30° N to 60° N) based on monthly means exhibited distinct seasonal cycles, with peak-to-peak amplitude of 7.15±0.22 ppm and 6.27±0.21 ppm, respectively. Nguyen et al. (2014) showed that XCO₂ estimated by CarbonTracker in the Northern Hemisphere has a seasonal variability with an amplitude of 3.2 ppm from 2009 to 2011. Further comparisons between our station, other TCCON stations and GOSAT and OCO-2 measurements are described further below. We conclude that the variation of XCO₂ in the Hefei area is in accord with the variation of other places in mid-latitude of Northern Hemisphere, both in trend and in phase. In our observations, the seasonal amplitude is larger than the results from other areas.

In the case of XCO, the individual value and daily average variation showed no obvious seasonal trend (Fig. 14). For daily average of XCO, day to day variations were considerable, ranging from 78.35 to 171.60 ppb. The seasonal cycle of monthly average XCO is not clearly discernible, because it is concealed by the large daily variability due to local influences. There is variability on seasonal timescale, showing the late autumn minimum and the spring maximum from Sep 2015 to March 2016. The main source for CO in this area is incomplete combustion of fossil fuels, so the seasonal behavior of XCO may reveal the trend of CO emission from vehicle exhaust. In recent publications of Liu et al. (2011), satellite measurements and model simulations showed that monthly mean of CO vertical column density had a maximum in winter and minimum in summer in the eastern area of China (20° N to 40° N, 107° E to 123° E) in 2004 and 2005. Angelbratt et al. (2011) estimated the trends of the CO partial columns from four European ground-based FTS stations, obtaining obvious seasonal variation during the year from 1996 to 2006. Also, in de Laat et al. (2010), the observations of ground-based spectrometers indicated that the



time series of CO total column in the Northern Hemisphere mid-latitude area had clear seasonal variations, with a wintertime maximum and summertime minimum due to photochemical reaction with OH radical for the 2003-2007 time period. However, in our observations, time series of individual XCO and their daily and monthly mean values showed no seasonal variation. The pattern may be due to the complicated emission of CO sources in Hefei area.

Further, diurnal variation can be obtained by analyzing data on a daily timescale. October 24, 2014 is selected because the data sampled on this clear sky day cover long daylight hours and are continuous. Figure 15 documents that total column of both species were higher at noon (UT+8), displaying similar behavior on this day. XCO₂ and XCO climbed to the maximum at noon, then dropped slowly until sunset. The prevailing wind direction on the day was from the southeast, resulting in urban regional emission superimposed on background. The midday peak for each gas reflects the influence of anthropogenic emissions.

Figure 16 presents the relationship between XCO₂ and XCO on daily scale, and the linear regression line shows the good correlation (correlation coefficient $R^2=0.60$) between them on October 24th. Atmospheric CO and CO₂ have common combustion sources. The strong correlation between CO₂ and CO indicates that there are strong influences of combustion emissions on CO₂. Also, the CO₂/CO correlation slope gives the emission ratio of CO₂ to CO, which varies with the sources of CO₂, depending on different combustion types and the biospheric activity. So the CO₂/CO correlation slope provides a characteristic signature of source regions and source type (Suntharalingam et al., 2004; Wang et al., 2010). From the study of Wang et al. (2010), the observed overall CO₂/CO ratio was in the range of 23-38 ppm/ppm in a rural site near Beijing in China during 2007-2008, which indicates the contribution of anthropogenic emissions and biospheric activities. In our case, the CO₂/CO correlation slope was 107 ppm/ppm On October 24, 2014.

However, both gases varied considerably between days, and some days saw weak correlation in variation of CO₂ and CO. So the entire data during the observations displayed weak correlation (not shown), and the correlation coefficient was 0.14 between daily average XCO₂ and XCO. Further, we analyzed the relationship of daily average XCO₂ and XCO on seasonal scale, found that although there was very weak correlation in summer and fall, there was strong correlation in winter and spring. Figure 17 is the plot of relationship between CO₂ and CO in winter and spring for 2014-2015 and 2015-2016. The high correlation coefficients suggest that combustion is an important source of CO₂ in winter and spring. Stable weather with strong inversion to prevent mixing and transport away from Hefei might also contribute to the correlation here. The correlation slope was 126.62 and 94.32 ppm/ppm, respectively, without considering the data in summer and fall. The values are larger than the reported values in Beijing (Wang et al., 2010 and references therein), primarily attributed to the smaller emission in CO.

5.4 Comparison with nearby TCCON's observations

We compare our data with similar ground-based high resolution observations from



320 Japanese Tsukuba TCCON station ($36^{\circ} 5' N$, $140^{\circ} 7' E$), because Tsukuba station
is the nearest station from our site and at similar latitude. Figure 18 provides time
series of individual measurements, daily averages and monthly averages of XCO_2 for
Tsukuba station from July 2014 to April 2016 and may be compared to Fig. 13. As can
be seen, XCO_2 exhibited a seasonal cycle, similar to that of our site (Fig. 13). The
325 lowest XCO_2 appeared in late summer (September), and the highest value was in
spring (April), which is the same as our XCO_2 data. The seasonal amplitude is 8.74
and 9.27 ppm in the year 2014-2015 and 2015-2016 from monthly average,
respectively, which is comparable to the corresponding values in our site.

XCO of Tsukuba station varied substantially between days, with daily average
between 71.69 to 144.57 ppb (Fig. 19), falling in the range of our daily average value.
330 The daily average plot showed large scatter with seasonal variation. The monthly
average XCO in Tsukuba area from July 2014 through April 2015 showed weak
seasonal variation, but April 2015 to April 2016 saw the clear seasonal variation. The
largest XCO was in spring (April) and the lowest value in fall (October), and this
variation is similar to that of XCO_2 at Tsukuba station. The seasonal amplitude is
335 27.21 ppb. The CO variability is driven by local effects (for example combustion
source) rather than global-scale effects for CO_2 , so the variation of CO in Tsukuba
looks different from that in Hefei.

5.5 Comparison with satellite data

To further evaluate the quality of our retrieved data, we made use of satellite
340 measurements to compare with the results. GOSAT and OCO-2 are currently the only
dedicated satellites mapping global atmospheric column amounts of CO_2 . Common
targets of both satellite missions are observation of XCO_2 . For the comparison with
ground-based FTS measurements, GOSAT Level 2 and OCO-2 Level 2 data within 4°
latitude/longitude radius of Hefei station were adopted. We set the collocation time to
345 1 day. The data are filtered as summarized in Table 4.

In order to directly compare two measurements made by different remote-sensing
instruments, their different a priori profiles and averaging kernels must be taken into
account (Rodgers and Connor, 2003). In Nguyen et al. (2014), TCCON data were
corrected by column averaging kernel of GOSAT retrievals, showing that the standard
350 deviation of the difference between non-corrected and corrected TCCON data is 0.24
ppm. In Wunch et al. (2011b), smoothing the TCCON profiles with the ACOS-GOSAT
averaging kernel at Lamont results in a bias of about 0.6 ppm. Zhou et al. (2016)
applied a priori profile of TCCON data to correct the satellite retrievals, found that the
difference between a priori-corrected and original satellite XCO_2 ranged from -0.6 to
355 0.3 ppm. Ohyama et al. (2015) used a common a priori profile and column averaging
kernel corrections, found that the effects of differences in a priori profile and column
averaging kernel are small. The average differences between the adjusted and the
original GOSAT XCO_2 data is -0.02 ± 0.17 ppm, and the average difference between
the smoothed and original TCCON XCO_2 data is -0.08 ± 0.12 ppm. The results
360 indicate that the impact of applying or not applying the a priori profiles and averaging
kernels for XCO_2 comparisons is small compared to difference between satellite and



FTS data. However it is not trivial to consider averaging kernels for comparison of different remote sensing observations, this requires actual variability of CO₂ profiles, which is unknown for our site at present. Therefore we compared the satellite and FTS data directly, without considering the effect of different a priori profiles and averaging kernels.

Comparison of daily and monthly average XCO₂ were carried out, because the temporal coverage is substantially different between our ground-based measurement and space-based observations. Figure 20 provides the direct comparison of our data with respect to co-located GOSAT data. Although not all FTS spectra were collected for GOSAT overpass, it is found that our daily average XCO₂ data are in broad agreement with the GOSAT data. The mean difference between satellite XCO₂ and ground-based FTS XCO₂ are computed as bias (satellite data minus FTS data), and the standard deviation of the differences are also calculated. There are 38 pairs of data for daily average XCO₂, giving a negative bias of -0.64 ppm and standard deviation of 1.27 ppm. As for monthly average XCO₂, 15 GOSAT data points can be compared to the corresponding ground-based FTS data. However, there exists an obvious discrepancy in July 2014 and August 2014 because of the sparse data of our FTS measurement or GOSAT overpass, so the data in the two months are not considered. The remaining 13 pairs of data give a mean bias of -0.49 ppm and standard deviation of 1.12 ppm. The correlation coefficients (R²) are 0.87 and 0.92 for daily average and monthly average values, respectively. Figure 21 is a scatter graph of the retrieval results of GOSAT and FTS, showing a good linear relationship. Therefore, our FTS data are in good agreement with the GOSAT data.

Morino et al. (2011) validated GOSAT XCO₂ and XCH₄ data with ground-based FTS data from 9 TCCON stations, and showed that the mean difference between the satellite XCO₂ data and FTS data were -8.85 ± 4.75 ppm, with a correlation coefficient of 0.378. Using a new GOSAT retrieval algorithm, Yoshida et al. (2013) improved the XCO₂ retrieval from GOSAT, achieving negative biases of -1.48 ppm and standard deviations of 2.09 ppm compared to TCCON data. Guerlet et al. (2013) compared GOSAT XCO₂ data using cloud and aerosol filters in the retrieval with co-located TCCON measurements, displaying a mean bias of -1.4 ± 2.5 ppm. Dils et al. (2014) showed that the satellite XCO₂ data retrieved by two different algorithms relative to FTS data produced a mean bias of -0.76 ± 2.37 ppm and -0.57 ± 2.50 ppm, respectively. Nguyen et al. (2014) found that XCO₂ data from GOSAT retrievals compared to ground-based XCO₂ TCCON measurement using three co-location methodologies displayed a positive bias in the range of 0.39 ppm to 4.07 ppm, with standard deviations of 0.39 ppm to 2.37 ppm, and the correlation coefficient from 0 to 0.90. In recent studies of Heymann et al. (2015), Ohyama et al. (2015) and Kulawik et al. (2016), the comparison results also demonstrate the good consistency between GOSAT XCO₂ and TCCON XCO₂. They found that the average differences between TANSO-FTS and ground-based FTS data were -0.34 ± 1.37 ppm, 0.40 ± 2.51 ppm and 0.48 ± 1.68 ppm, with correlation coefficients of 0.86, 0.87 and 0.74. So the average differences between TANSO-FTS and our FTS data and standard deviations of the differences are within the range of comparison results from other TCCON site data,



and the correlation coefficients are comparable to that of other comparison results. Then we used OCO-2 version 7Br data (bias-corrected Lite File product) for comparison. Figure 22 presents the comparison of our data with respect to OCO-2 data. There are 55 daily average OCO-2 data that can be compared to the
410 corresponding ground-based FTS data, yielding a positive bias of 1.00 ppm and standard deviation of 1.92 ppm. Additionally, 16 monthly average OCO-2 data are available for comparison with FTS data, producing a positive bias of 1.07 ppm and standard deviation of 1.62 ppm. The correlation coefficients (R^2) are 0.81 and 0.85 for the daily average and monthly average XCO_2 , respectively. The differences between
415 FTS and OCO-2 data are larger than those of FTS and GOSAT. Figure 23 is scatter graph for retrieval results of OCO-2 and FTS, displaying a fairly good linear relationship. In fact, we also compared OCO-2 version 7r data (without bias correction) with our FTS data. It is unexpected that the bias-corrected OCO-2 data show larger differences than OCO-2 data without bias correction, and the latter have a
420 bias of -0.15 ± 1.79 ppm and 0.14 ± 1.53 ppm for daily average and monthly average comparison (not shown).

In recent studies of Wunch et al. (2016), they compared the OCO-2 version 7Br data with ground-based TCCON data, showing that the median differences between OCO-2 and TCCON data were less than 0.5 ppm, with the RMS differences below
425 1.5ppm and correlation coefficients from 0.50 to 0.75 for ocean glint mode, land glint mode and nadir mode. For our comparison, the correlations are slightly better than that of other comparison results, while the differences of bias-corrected OCO-2 data from our FTS data and standard deviations are larger than those of other TCCON site data. The comparison results demonstrated that our ground-based FTS measurements
430 are broadly consistent with the OCO-2 observations.

6. Conclusions

A solar observatory deployed at Hefei China has collected near infrared solar spectra since July 2014. Total columns of atmospheric CO_2 and CO have been successfully
435 retrieved from high resolution ground-based FTS measurements. The spectra collected using an InSb detector in the first year were compared with those collected by an InGaAs detector in the second year, showing that InGaAs spectra have approximately two-times better signal-to-noise ratios, and correspondingly smaller RMS spectral fitting residuals compared to InSb spectra. Consequently, the measurement precision of retrieved XCO_2 and XCO for InGaAs spectra is superior to
440 InSb spectra, with about 0.04 % and 0.09 % for XCO_2 , 1.07 % and 2.00 % for XCO within clear sky days, respectively. Daily and monthly averaged values for XCO_2 showed an obvious seasonal cycle, while daily and monthly average of XCO displayed no clearly seasonal variation. Further, we analyzed the relationship of daily average XCO_2 and XCO on seasonal scale, found that although there was very weak
445 correlation between them in summer and fall, there existed strong correlation in winter and spring. The CO_2/CO correlation slope was 126.62 and 94.32 ppm/ppm in winter and spring for 2014-2015 and 2015-2016, respectively, larger than the reported values in Beijing, China. Ground-based observations from the Japanese Tsukuba



TCCON station were used to compare with our observations, the results showed that
450 the variation phase and seasonal amplitude of XCO₂ are similar to our results, but the
variation of XCO in Tsukuba looks different from our data in Hefei. The direct
comparison of GOSAT data with our FTS results suggests that daily average and
monthly average XCO₂ are in good agreement, giving a bias of -0.64 ppm and -0.49
455 ppm, with standard deviation of 1.27 ppm and 1.12 ppm, respectively. The correlation
coefficient (R^2) is 0.87 and 0.92 for the daily and monthly average XCO₂ between our
FTS measurement and GOSAT observations, respectively. Daily average OCO-2 data
produce a positive bias of 1.00 ppm and standard deviation of 1.92 ppm relative to
ground-based data, and the monthly average OCO-2 data give a positive bias of 1.07
460 ppm and standard deviation of 1.62 ppm. Our daily and monthly average XCO₂ show
strong correlation with OCO-2 observations, with correlation coefficient (R^2) of 0.81
and 0.85, respectively. The results show that our observations using ground-based
FTS are well consistent with the GOSAT and OCO-2 observations. The comparison
results have demonstrated the ability of our ground-based FTS to detect daily
465 variations and reveal seasonal changes of atmospheric CO₂ and CO, also the ability to
validate the satellite observations. It is important that Hefei site can discern the
Northern hemisphere seasonal cycle of CO₂ with the late summer minimum.
The observations described here present a means of precise remote sensing of
atmospheric constituents in the Hefei area. Column values obtained from this site will
470 help to determine the CO₂ and CO sources and sinks in east of China, where
measurements are currently scarce. However, the results derived here need to be
calibrated to the World Meteorological Organization's (WMO) gas scale. We have not
yet calibrated our data by measurements of instrument aboard aircraft or
balloon-borne AirCore system. The improvements will enhance the level of accuracy
475 in the near future. Therefore, further research is to utilize in situ measurements or
model simulation to verify the observation.

Acknowledgement. We gratefully acknowledge the support of National Natural
Science Foundation of China (41405134; 41575021; 91544212; 41605018), the
480 National Key Technology R&D Program of China (2016YFC0200800), and Anhui
Province Natural Science Foundation of China (Grant NO. 1308085MD79) for
conducting this research. We thank the members of GOSAT Project for providing us
with GOSAT L2 data products. We also thank the members of OCO Project for
providing OCO-2 L2 data. We very appreciate the technical help from Institute of
Environmental Physics, University of Bremen, Germany and Karlsruhe Institute of
485 Technology (KIT), Institute for Meteorology and Climate Research (IMK-ASF),
Karlsruhe, Germany.

References

490 Angelbratt, J., Mellqvist, J., Simpson, D., Jonson, J.E., Blumenstock, T., Borsdorff, T., Duchatelet,
P., Forster, F., Hase, F., Mahieu, E., De Mazière, M., Notholt, J., Petersen, A.K., Raffalski, U.,
Servais, C., Sussmann, R., Warneke, T., Vigouroux, C.: Carbon monoxide (CO) and ethane
(C₂H₆) trends from ground-based solar FTIR measurements at six European stations,



- comparison and sensitivity analysis with the EMEP model. *Atmos. Chem. Phys.*, 11, 9253-9269, doi:10.5194/acp-11-9253-2011, 2011.
- 495 Boesch, H., Baker, D., Connor, B., Crisp, D., and Miller, C.: Global Characterization of CO₂ Column Retrievals from Shortwave-Infrared Satellite Observations of the Orbiting Carbon Observatory-2 Mission, *Remote Sensing*, 3, 270–304, doi:10.3390/rs3020270, 2011.
- Bovensmann, H., Burrows, J. P., Buchwitz, M., Frerick, J., Noel, S., Rozanov, V. V., Chance, K. V., and Goede, A.: SCIAMACHY-Mission Objectives and Measurement Modes, *J. Atmos. Sci.*, 56, 127–150, 1999.
- 500 Bovensmann, H., Buchwitz, M., Frerick, J., Hoogeveen, R., Kleipool, Q., Lichtenberg, G., Noel, S., Richter, A., Rozanov, A., Rozanov, V. V., Skupin, J., von Savigny, C., Wuttke, M., and Burrows, J. P.: SCIAMACHY on ENVISAT: In-flight optical performance and first results, in: *Remote Sensing of Clouds and the Atmosphere VIII*, edited by: Schafer, K. P., Comeron, A., Carleer, M. R., and Picard, R. H., *Proc. of SPIE*, Vol. 5235, 160–173, 2004.
- 505 Buchholz, R.R., Paton-Walsh, C., Griffith, D.W.T., Kubistin, D., Caldow, C., Fisher, J.A., Deutscher, N.M., Kettlewell, G., Riggensbach, M., Macatangay, R., Krummel, P.B., Langenfelds, R.L.: Source and meteorological influences on air quality (CO, CH₄ & CO₂) at a Southern Hemisphere urban site, *Atmos. Environ.* 126, 274-289. doi: 10.1016/j.atmosenv.2015.11.041, 2016.
- 510 Butz, A., Guerlet, S., Hasekamp, O., Schepers, D., Galli, A., Aben, I., Frankenberg, C., Hartmann, J.-M., Tran, H., Kuze, A., Keppel-Aleks, G., Toon, G., Wunch, D., Wennberg, P., Deutscher, N., Griffith, D., Macatangay, R., Messerschmidt, J., Notholt, J., and Warneke, T.: Toward accurate CO₂ and CH₄ observations from GOSAT, *Geophys. Res. Lett.*, 38, L14812, doi:10.1029/2011GL047888, 2011.
- 515 Clerbaux, C., George, M., Turquety, S., Walker, K.A., Barret, B., Bernath, P., Boone, C., Borsdorff, T., Cammas, J.P., Catoire, V., Coffey, M., Coheur, P.F., Deeter, M., De Mazière, M., Drummond, J., Duchatelet, P., Dupuy, E., de Zafra, R., Eddounia, F., Edwards, D.P., Emmons, L., Funke, B., Gille, J., Griffith, D.W.T., Hannigan, J., Hase, F., Höpfner, M., Jones, N., Kagawa, A., Kasai, Y., Kramer, I., Le Flochmoën, E., Livesey, N.J., López-Puertas, M., Luo, M., Mahieu, E., Murtagh, D., Nédélec, P., Pazmino, A., Pumphrey, H., Ricaud, P., Rinsland, C.P., Robert, C., Schneider, M., Senten, C., Stiller, G., Strandberg, A., Strong, K., Sussmann, R., Thouret, V., Urban, J., Wiacek, A.: CO measurements from the ACE-FTS satellite instrument: data analysis and validation using ground-based, airborne and spaceborne observations. *Atmos. Chem. Phys.*, 8, 2569-2594. doi:10.5194/acp-8-2569-2008, 2008.
- 525 Crisp, D., Atlas, R. M., Breon, F.-M., Brown, L. R., Burrows, J. P., Ciais, P., Connor, B. J., Doney, S. C., Fung, I. Y., Jacob, D. J., Miller, C. E., O'Brien, D., Pawson, S., Randerson, J. T., Rayner, P., Salawitch, R. J., Sander, S. P., Sen, B., Stephens, G. L., Tans, P. P., Toon, G. C., Wennberg, P. O., Wofsy, S. C., Yung, Y. L., Kuang, Z., Chudasama, B., Sprague, G., Weiss, B., Pollock, R., Kenyon, D., and Schroll, S.: The Orbiting Carbon Observatory (OCO) mission, *Adv. Space Res.*, 34, 700-709, 2004.
- 530 de Laat, A.T.J., Gloudemans, A.M.S., Schrijver, H., Aben, I., Nagahama, Y., Suzuki, K., Mahieu, E., Jones, N.B., Paton-Walsh, C., Deutscher, N.M., Griffith, D.W.T., De Mazière, M., Mittermeier, R.L., Fast, H., Notholt, J., Palm, M., Hawat, T., Blumenstock, T., Hase, F., Schneider, M., Rinsland, C., Dzhola, A.V., Grechko, E.I., Poberovskii, A.M., Makarova, M.V., Mellqvist, J., Strandberg, A., Sussmann, R., Borsdorff, T., Rettinger, M.: Validation of five



- years (2003-2007) of SCIAMACHY CO total column measurements using ground-based spectrometer observations. *Atmos. Meas. Tech.* 3, 1457-1471. doi:10.5194/amt-3-1457-2010, 2010.
- 540 Deutscher, N.M., Griffith, D.W.T., Bryant, G.W., Wennberg, P.O., Toon, G.C., Washenfelder, R.A., Keppel-Aleks, G., Wunch, D., Yavin, Y., Allen, N.T., Blavier, J.F., Jim énez, R., Daube, B.C., Bright, A.V., Matross, D.M., Wofsy, S.C., Park, S.: Total column CO₂ measurements at Darwin, Australia – site description and calibration against in situ aircraft profiles. *Atmos. Meas. Tech.* 3, 947-958. doi:10.5194/amt-3-947-2010, 2010.
- 545 Dils, B., Buchwitz, M., Reuter, M., Schneising, O., Boesch, H., Parker, R., Guerlet, S., Aben, I., Blumenstock, T., Burrows, J. P., Butz, A., Deutscher, N. M., Frankenberg, C., Hase, F., Hasekamp, O. P., Heymann, J., DeMazi ère, M., Notholt, J., Sussmann, R., Warneke, T., Griffith, D., Sherlock, V., and Wunch, D.: The Greenhouse Gas Climate Change Initiative (GHG-CCI): comparative validation of GHG-CCI SCIAMACHY/ENVISAT and
- 550 TANSO-FTS/GOSAT CO₂ and CH₄ retrieval algorithm products with measurements from the TCCON, *Atmos. Meas. Tech.*, 7, 1723–1744, doi:10.5194/amt-7-1723-2014, 2014.
- Dohe, S., 2013. Measurements of atmospheric CO₂ columns using ground-based FTIR spectra. Doctoral thesis, Karlsruhe Institute of Technology.
- Frankenberg, C., Pollock, R., Lee, R.A.M., Rosenberg, R., Blavier, J.F., Crisp, D., O'Dell, C.W.,
- 555 Osterman, G.B., Roehl, C., Wennberg, P.O., Wunch, D.: The Orbiting Carbon Observatory (OCO-2): spectrometer performance evaluation using pre-launch direct sun measurements. *Atmos. Meas. Tech.* 8, 301-313. doi:10.5194/amt-8-301-2015, 2015.
- Hamazaki, T., Kaneko, Y., Kuze, A., and Kondo, K.: Fourier transform spectrometer for greenhouse gases observing satellite (GOSAT), in: Enabling Sensor and Platform
- 560 Technologies for Spaceborne Remote Sensing, edited by Komar, G.J., Wang, J., Kimura, T., *Proc. of SPIE*, vol. 5659, 73-80, doi: 10.1117/12.581198, 2005.
- Hase, F., Blumenstock, T., and Paton-Walsh, C.: Analysis of the instrumental line shape of high resolution Fourier transform IR spectrometers with gas cell measurements and new retrieval software, *Appl. Optics*, 38, 3417–3422, doi:10.1364/AO.38.003417, 1999.
- 565 Hase, F., Drouin, B. J., Roehl, C. M., Toon, G. C., Wennberg, P. O., Wunch, D., Blumenstock, T., Desmet, F., Feist, D. G., Heikkinen, P., De Mazi ère, M., Rettinger, M., Robinson, J., Schneider, M., Sherlock, V., Sussmann, R., Té Y., Warneke, T., and Weinzierl, C.: Calibration of sealed HCl cells used for TCCON instrumental line shape monitoring, *Atmos. Meas. Tech.*, 6, 3527–3537, doi:10.5194/amt-6-3527-2013, 2013.
- 570 Heymann, J., Reuter, M., Hilker, M., Buchwitz, M., Schneising, O., Bovensmann, H., Burrows, J. P., Kuze, A., Suto, H., Deutscher, N. M., Dubey, M. K., Griffith, D. W. T., Hase, F., Kawakami, S., Kivi, R., Morino, I., Petri, C., Roehl, C., Schneider, M., Sherlock, V., Sussmann, R., Velasco, V. A., Warneke, T., and Wunch, D.: Consistent satellite XCO₂ retrievals from SCIAMACHY and GOSAT using the BESD algorithm, *Atmos. Meas. Tech.*, 8,
- 575 2961–2980, doi:10.5194/amt-8-2961-2015, 2015.
- Guerlet, S., Butz, A., Schepers, D., Basu, S., Hasekamp, O. P., Kuze, A., Yokota, T., Blavier, J.-F., Deutscher, N. M., Griffith, D. W. T., Hase, F., Kyro, E., Morino, I., Sherlock, V., Sussmann, R., Galli, A., and Aben, I.: Impact of aerosols and thin cirrus on retrieving and validating XCO₂ from GOSAT shortwave infrared measurements, *J. Geophys. Res.-Atmos.*, 118,
- 580 4887–4905, doi:10.1002/jgrd.50332, 2013.



- IPCC, 2014: Climate Change 2014: Synthesis Report. Contribution of Working Groups I, II and III to the Fifth Assessment Report of the Intergovernmental Panel on Climate Change [Core Writing Team, R.K. Pachauri and L.A. Meyer (eds.)]. IPCC, Geneva, Switzerland, 151 pp.
- 585 Kiel, M., Wunch, D., Wennberg, P. O., Toon, G. C., Hase, F., and Blumenstock, T.: Improved retrieval of gas abundances from near-infrared solar FTIR spectra measured at the Karlsruhe TCCON station, *Atmos. Meas. Tech.*, 9, 669–682, doi:10.5194/amt-9-669-2016, 2016a.
- Kiel, M., Hase, F., Blumenstock, T., and Kirner, O.: Comparison of XCO abundances from the Total Carbon Column Observing Network and the Network for the Detection of Atmospheric Composition Change measured in Karlsruhe, *Atmos. Meas. Tech.*, 9, 2223–2239, doi:10.5194/amt-9-2223-2016, 2016b.
- 590 Kulawik, S., Wunch, D., O'Dell, C., Frankenberg, C., Reuter, M., Oda, T., Chevallier, F., Sherlock, V., Buchwitz, M., Osterman, G., Miller, C. E., Wennberg, P. O., Griffith, D., Morino, I., Dubey, M. K., Deutscher, N. M., Notholt, J., Hase, F., Warneke, T., Sussmann R., Robinson, J., Strong, K., Schneider, M., De Mazière, M., Shiomi, K., Feist, D. G., Iraci, L.
- 595 T., and Wolf, J.: Consistent evaluation of ACOS-GOSAT, BESD-SCIAMACHY, CarbonTracker, and MACC through comparisons to TCCON. *Atmos. Meas. Tech.*, 9, 683–709, doi:10.5194/amt-9-683-2016, 2016.
- Kuze, A., Suto, H., Nakajima, M., and Hamazaki, T.: Thermal and near infrared sensor for carbon observation Fourier-transform spectrometer on the Greenhouse Gases Observing Satellite for greenhouse gases monitoring, *Appl. Optics*, 48, 6716–6733, 2009.
- 600 Le Quéré C., Peters, G.P., Andres, R.J., Andrew, R.M., Boden, T.A., Ciais, P., Friedlingstein, P., Houghton, R.A., Marland, G., Moriarty, R., Sitch, S., Tans P., Arneeth, A., Arvanitis, A., Bakker, D.C.E., Bopp, L., Canadell, J. G., Chini, L.P., Doney, S.C., Harper, A., Harris, I., House, J.I., Jain, A.K., Jones, S.D., Kato, E., Keeling, R.F., Klein Goldewijk, K., Körtzinger, A., Koven, C., Lefèvre, N., Maignan, F., Omar, A., Ono, T., Park, G.-H., Pfeil, B., Poulter, B., Raupach, M.R., Regnier, P., Rödenbeck, C., Saito, S., Schwinger, J., Segschneider, J., Stocker, B.D., Takahashi, T., Tilbrook, B., van Heuven, S., Viovy, N., Wanninkh, R., Wiltshire, A., and Zaehle, S.: The global carbon budget 2013. *Earth Syst. Sci. Data* 6, 235–263. doi:10.5194/essd-6-235-2014, 2014.
- 610 Lindqvist, H., O'Dell, C. W., Basu, S., Boesch, H., Chevallier, F., Deutscher, N., Feng, L., Fisher, B., Hase, F., Inoue, M., Kivi, R., Morino, I., Palmer, P. I., Parker, R., Schneider, M., Sussmann, R., and Yoshida, Y.: Does GOSAT capture the true seasonal cycle of carbon dioxide?, *Atmos. Chem. Phys.*, 15, 13023–13040, doi:10.5194/acp-15-13023-2015, 2015.
- 615 Liu, C., Beirle, S., Butler, T., Liu, J., Hoor, P., Jöckel, P., Penning de Vries, M., Pozzer, A., Frankenberg, C., Lawrence, M.G., Lelieveld, J., Platt, U., and Wagner, T.: Application of SCIAMACHY and MOPITT CO total column measurements to evaluate model results over biomass burning regions and Eastern China. *Atmos. Chem. Phys.* 11, 6083–6114. doi:10.5194/acp-11-6083-2011, 2011.
- Messerschmidt, J., Macatangay, R., Notholt, J., Petri, C., Warneke T., and Weinzierl, C.: Side by side measurements of CO₂ by ground-based Fourier transform spectrometry (FTS), *Tellus B*, 62, 749–758, doi:10.1111/j.1600-0889.2010.00491.x, 2010.
- 620 Messerschmidt, J., Geibel, M.C., Blumenstock, T., Chen, H., Deutscher, N.M., Engel, A., Feist, D.G., Gerbig, C., Gisi, M., Hase, F., Katrynski, K., Kolle, O., Lavrič, J.V., Notholt, J., Palm, M., Ramonet, M., Rettinger, M., Schmidt, M., Sussmann, R., Toon, G.C., Truong, F.,



- 625 Warneke, T., Wennberg, P.O., Wunch, D., and Xueref-Remy, I.: Calibration of TCCON column-averaged CO₂: the first aircraft campaign over European TCCON sites. *Atmos. Chem. Phys.* 11, 10765-10777. doi:10.5194/acp-11-10765-2011, 2011.
- Morino, I., Uchino, O., Inoue, M., Yoshida, Y., Yokota, T., Wennberg, P. O., Toon, G. C., Wunch, D., Roehl, C. M., Notholt, J., Warneke, T., Messerschmidt, J., Griffith, D. W. T., Deutscher, N. M., Sherlock, V., Connor, B., Robinson, J., Sussmann, R., and Rettinger, M.: Preliminary validation of column-averaged volume mixing ratios of carbon dioxide and methane retrieved from GOSAT short-wavelength infrared spectra, *Atmos. Meas. Tech.*, 4, 1061–1076, doi:10.5194/amt-4-1061-2011, 2011.
- 630 Newman, S., Jeong, S., Fischer, M.L., Xu, X., Haman, C.L., Lefter, B., Alvarez, S., Rappenglueck, B., Kort, E.A., Andrews, A.E., Peischl, J., Gurney, K.R., Miller, C.E., and Yung, Y.L.: Diurnal tracking of anthropogenic CO₂ emissions in the Los Angeles basin megacity during spring 2010. *Atmos. Chem. Phys.* 13, 4359-4372. doi:10.5194/acp-13-4359-2013, 2013.
- Nguyen, H., Osterman, G., Wunch, D., O'Dell, C., Mandrake, L., Wennberg, P., Fisher, B., and Castano, R.: A method for collocating satellite XCO₂ data to ground-based data and its application to ACOS-GOSAT and TCCON. *Atmos. Meas. Tech.* 7, 2631-2644. doi:10.5194/amt-7-2631-2014, 2014.
- 640 Ohyama, H., Kawakami, S., Tanaka, T., Morino, I., Uchino, O., Inoue, M., Sakai, T., Nagai, T., Yamazaki, A., Uchiyama, A., Fukamachi, T., Sakashita, M., Kawasaki, T., Akaho, T., Arai, K., and Okumura, H. : Observations of XCO₂ and XCH₄ with ground-based high-resolution FTS at Saga, Japan and comparisons with GOSAT products. *Atmos. Meas. Tech.*, 8, 5263–5276. doi:10.5194/amt-8-5263-2015, 2015.
- 645 Olsen, S.C., Randerson, J.T.: Differences between surface and column atmospheric CO₂ and implications for carbon cycle research. *Journal of Geophysical Research: Atmospheres* 109. doi:10.1029/2003JD003968, 2004.
- 650 Reuter, M., Bovensmann, H., Buchwitz, M., Burrows, J. P., Connor, B. J., Deutscher, N. M., Griffith, D. W. T., Heymann, J., Keppel-Aleks, G., Messerschmidt, J., Notholt, J., Petri, C., Robinson, J., Schneising, O., Sherlock, V., Velasco, V., Warneke, T., Wennberg, P. O., Wunch, D.: Retrieval of atmospheric CO₂ with enhanced accuracy and precision from SCIAMACHY: Validation with FTS measurements and comparison with model results, *J. Geophys. Res.-Atmos.*, 116, D04301, doi:10.1029/2010JD015047, 2011.
- 655 Rodgers, C. D. and Connor, B. J.: Intercomparison of remote sounding instruments, *J. Geophys. Res. Atmos.*, 108, 4116, doi:10.1029/2002JD002299, 2003.
- Rokotyan, N.V., Zakharov, V.I., Griбанov, K.G., Schneider, M., Bréon, F.M., Jouzel, J., Imasu, R., Werner, M., Butzin, M., Petri, C., Warneke, T., and Notholt, J.: A posteriori calculation of δ¹⁸O and δD in atmospheric water vapour from ground-based near-infrared FTIR retrievals of H₂16O, H₂18O, and HD₁₆O. *Atmos. Meas. Tech.* 7, 2567-2580. doi:10.5194/amt-7-2567-2014, 2014.
- 660 Rokotyan, N.V., Imasu, R., Zakharov, V.I., Griбанov, K.G., and Khamaturova, M.Y.: The amplitude of the CO₂ seasonal cycle in the atmosphere of the Ural region retrieved from ground-based and satellite near-IR measurements. *Atmos Ocean Opt* 28, 49-55. doi:10.1134/S102485601501011X, 2015.
- 665 Sarangi, T., Naja, M., Ojha, N., Kumar, R., Lal, S., Venkataramani, S., Kumar, A., Sagar, R., Chandola, H.C.: First simultaneous measurements of ozone, CO, and NO_y at a high-altitude



- regional representative site in the central Himalayas. *J. Geophys. Res. Atmos.* 119, 1592-1611. doi:10.1002/2013JD020631, 2014.
- 670 Schibig, M. F., Steinbacher, M., Buchmann, B., van der LaanLuijkx, I. T., van der Laan, S., Ranjan, S., and Leuenberger, M. C.: Comparison of continuous in situ CO₂ observations at Jungfrauoch using two different measurement techniques, *Atmos. Meas. Tech.*, 8, 57–68, doi:10.5194/amt-8-57-2015, 2015.
- 675 Schneising, O., Bergamaschi, P., Bovensmann, H., Buchwitz, M., Burrows, J. P., Deutscher, N. M., Griffith, D. W. T., Heymann, J., Macatangay, R., Messerschmidt, J., Notholt, J., Rettinger, M., Reuter, M., Sussmann, R., Velazco, V. A., Warneke, T., Wennberg, P. O., and Wunch, D.: Atmospheric greenhouse gases retrieved from SCIAMACHY: comparison to ground-based FTS measurements and model results, *Atmos. Chem. Phys.*, 12, 1527–1540, doi:10.5194/acp-12-1527-2012, 2012.
- 680 Schneising, O., Reuter, M., Buchwitz, M., Heymann, J., Bovensmann, H., Burrows, J.P.: Terrestrial carbon sink observed from space: variation of growth rates and seasonal cycle amplitudes in response to interannual surface temperature variability. *Atmos. Chem. Phys.* 14, 133-141. doi:10.5194/acp-14-133-2014, 2014.
- 685 Suntharalingam, P., Jacob, D. J., Palmer, P. I., Logan, J. A., Yantosca, R. M., Xiao, Y. P., Evans, M. J., Streets, D. G., Vay, S. L., and Sachse, G. W.: Improved quantification of Chinese carbon fluxes using CO₂/CO correlations in Asian outflow, *J. Geophys. Res.-Atmos.*, 109, D18S18, doi:10.1029/2003JD004362, 2004.
- Toon, G., Blavier, J.-F., Washenfelder, R., Wunch, D., Keppel-Aleks, G., Wennberg, P., Connor, B., Sherlock, V., Griffith, D., Deutscher, N., Notholt, J.: Total Column Carbon Observing Network (TCCON), *Advances in Imaging. Optical Society of America, Vancouver*, p. JMA3. doi:10.1364/FTS.2009.JMA3, 2009.
- 690 Vardag, S. N., Hammer, S., O'Doherty, S., Spain, T. G., Wastine, B., Jordan, A., and Levin, I.: Comparisons of continuous atmospheric CH₄, CO₂ and N₂O measurements – results from a travelling instrument campaign at Mace Head, *Atmos. Chem. Phys.*, 14, 8403–8418, doi:10.5194/acp-14-8403-2014, 2014.
- 695 Wang, Y., Munger, J. W., Xu, S., McElroy, M. B., Hao, J., Nielsen, C. P., and Ma, H.: CO₂ and its correlation with CO at a rural site near Beijing: implications for combustion efficiency in China, *Atmos. Chem. Phys.*, 10, 8881–8897, doi:10.5194/acp-10-8881-2010, 2010.
- 700 Wang, Z., Deutscher, N. M., Warneke, T., Notholt, J., Dils, B., Griffith, D.W.T., Schmidt, M., Ramonet, M., and Gerbig, C.: Retrieval of tropospheric column-averaged CH₄ mole fraction by solar absorption FTIR-spectrometry using N₂O as a proxy. *Atmos. Meas. Tech.* 7, 3295-3305. doi:10.5194/amt-7-3295-2014, 2014.
- Washenfelder, R. A., Toon, G. C., Blavier, J.-F., Yang, Z., Allen, N. T., Wennberg, P. O., Vay, S. A., Matross, D. M., and Daube, B. C.: Carbon dioxide column abundances at the Wisconsin Tall Tower site, *J. Geophys. Res.-Atmos.*, 111, D22305, doi:10.1029/2006JD007154, 2006.
- 705 WMO: 17th WMO/IAEA Meeting on Carbon Dioxide, Other Greenhouse Gases and Related Tracers Measurement Techniques (GGMT-2013), Beijing, China, 10-13 June 2013, GAW Report No. 213, World Meteorological Organization, 30 Geneva, Switzerland, 2014.
- 710 Wunch, D., Toon, G.C., Wennberg, P.O., Wofsy, S.C., Stephens, B.B., Fischer, M.L., Uchino, O., Abshire, J.B., Bernath, P., Biraud, S.C., Blavier, J.F.L., Boone, C., Bowman, K.P., Browell, E.V., Campos, T., Connor, B.J., Daube, B.C., Deutscher, N.M., Diao, M., Elkins, J.W., Gerbig,



- 715 C., Gottlieb, E., Griffith, D.W.T., Hurst, D.F., Jiménez, R., Keppel-Aleks, G., Kort, E.A.,
 Macatangay, R., Machida, T., Matsueda, H., Moore, F., Morino, I., Park, S., Robinson, J.,
 Roehl, C.M., Sawa, Y., Sherlock, V., Sweeney, C., Tanaka, T., and Zondlo, M.A.: Calibration
 of the Total Carbon Column Observing Network using aircraft profile data. *Atmos. Meas.*
Tech. 3, 1351-1362. doi:10.5194/amt-3-1351-2010, 2010.
- 720 Wunch, D., Toon, G. C., Blavier, J.-F. L., Washenfelder, R. A., Notholt, J., Connor, B. J., Griffith,
 D. W. T., Sherlock, V., and Wennberg, P. O.: The Total Carbon Column Observing Network,
Philos. T. Roy. Soc. A, 369, 2087–2112, doi:10.1098/rsta.2010.0240, 2011a.
- 725 Wunch, D., Wennberg, P.O., Toon, G.C., Connor, B.J., Fisher, B., Osterman, G.B., Frankenberg, C.,
 Mandrake, L., O'Dell, C., Ahonen, P., Biraud, S.C., Castano, R., Cressie, N., Crisp, D.,
 Deutscher, N.M., Eldering, A., Fisher, M.L., Griffith, D.W.T., Gunson, M., Heikkinen, P.,
 Keppel-Aleks, G., Kyrö E., Lindenmaier, R., Macatangay, R., Mendonca, J., Messerschmidt,
 J., Miller, C.E., Morino, I., Notholt, J., Oyafuso, F.A., Rettinger, M., Robinson, J., Roehl,
 C.M., Salawitch, R.J., Sherlock, V., Strong, K., Sussmann, R., Tanaka, T., Thompson, D.R.,
 Uchino, O., Warneke, T., and Wofsy, S.C.: A method for evaluating bias in global
 measurements of CO₂ total columns from space. *Atmos. Chem. Phys.* 11, 12317-12337.
 doi:10.5194/acp-11-12317-2011, 2011b.
- 730 Wunch, D., Toon, G. C., Sherlock, V., Deutscher, N. M., Liu, X., Feist, D. G., and Wennberg, P. O.:
 The Total Carbon Column Observing Network's GGG2014 Data Version. Carbon Dioxide
 Information Analysis Center, Oak Ridge National Laboratory, Oak Ridge, Tennessee, USA,
 available at: doi:10.14291/tcon.ggg2014.documentation.R0/1221662, 2015.
- 735 Wunch, D., Wennberg, P.O., Osterman, G., Fisher, B., Naylor, B., Roehl, C. M., O'Dell, C.,
 Mandrake, L., Viatte, C., Griffith, D. W. T., Deutscher, N. M., Velasco, V. A., Notholt,
 J., Warneke, T., Petri, C., Maziere, M. De, Sha, M. K., Sussmann, R., Rettinger, M., Pollard, D.,
 Robinson, J., Morino, I., Uchino O., Hase, F., Blumenstock, T., Kiel, M., Feist, D. G., Arnold
 S.G., Strong, K., Mendonca, J., Kivi, R., Heikkinen, P., Iraci, L., Podolske, J., Hillyard, P. W.,
 Kawakami, S., Dubey, M. K., Parker, H. A., Sepulveda, E., Rodriguez, O. E. G., Te, Y.,
 740 Jeseck, P., Gunson, M. R., Crisp, D., and Eldering A., Comparisons of the Orbiting Carbon
 Observatory-2 (OCO-2) XCO₂ measurements with TCCON, *Atmos. Meas. Tech. Discuss.*,
 doi:10.5194/amt-2016-227, 2016.
- 745 Yang, Z., Toon, G.C., Margolis, J.S., and Wennberg, P.O.: Atmospheric CO₂ retrieved from
 ground-based near IR solar spectra. *Geophysical Research Letters* 29, 53-51-53-54.
 doi:10.1029/2001GL014537, 2002.
- Yang, Z., Wennberg, P.O., Cageao, R.P., Pongetti, T.J., Toon, G.C., and Sander, S.P.: Ground-based
 photon path measurements from solar absorption spectra of the O₂ A-band. *Journal of*
Quantitative Spectroscopy and Radiative Transfer 90, 309-321.
 doi:http://dx.doi.org/10.1016/j.jqsrt.2004.03.020, 2005.
- 750 Yin, Y., Chevallier, F., Ciais, P., Broquet, G., Fortems-Cheiney, A., Pison, I., Saunoy, M.:
 Decadal trends in global CO emissions as seen by MOPITT. *Atmos. Chem. Phys.* 15,
 13433-13451. doi:10.5194/acp-15-13433-2015, 2015.
- 755 Yoshida, Y., Kikuchi, N., Morino, I., Uchino, O., Oshchepkov, S., Bril, A., Saeki, T., Schutgens, N.,
 Toon, G. C., Wunch, D., Roehl, C. M., Wennberg, P. O., Griffith, D. W. T., Deutscher, N. M.,
 Warneke, T., Notholt, J., Robinson, J., Sherlock, V., Connor, B., Rettinger, M., Sussmann, R.,
 Ahonen, P., Heikkinen, P., Kyrö E., Mendonca, J., Strong, K., Hase, F., Dohe, S., and Yokota,



- T.: Improvement of the retrieval algorithm for GOSAT SWIR XCO₂ and XCH₄ and their validation using TCCON data, Atmos. Meas. Tech., 6, 1533–1547, doi:10.5194/amt-6-1533-2013, 2013.
- 760 Zhou, M., Dils, B., Wang, P., Detmers, R., Yoshida, Y., O'Dell, C. W., Feist, D. G., Velazco, V. A., Schneider, M., and Maziere, M. De, Validation of TANSO-FTS/GOSAT XCO₂ and XCH₄ glint mode retrievals using TCCON data from near-ocean sites, Atmos. Meas. Tech., 9, 1415–1430, doi:10.5194/amt-9-1415-2016, 2016.

Table 1. Spectral windows for retrieval of column of CO₂, CO and O₂.

Gas	Center of spectral window (cm ⁻¹)	Width (cm ⁻¹)	Interfering gas
CO ₂	6220.0	80.0	H ₂ O, HDO, CH ₄
CO ₂	6339.5	85.0	H ₂ O, HDO
CO	4233.0	48.6	CH ₄ , H ₂ O, HDO
CO	4290.4	56.8	CH ₄ , H ₂ O, HDO
O ₂	7885.0	240.0	H ₂ O, HF, CO ₂

Table 2. The signal-to-noise ratio and spectral fitting of InGaAs spectra compared with InSb spectra for different spectral windows.

Gas	spectral window (cm ⁻¹)	SNR of InGaAs	SNR of InSb	RMS fitting residual of InGaAs	RMS fitting residual of InSb
CO ₂	6180-6260	1050	320	0.19%	0.32%
CO ₂	6297-6382	997	320	0.21%	0.31%
CO	4208-4257	1060	233	0.50%	0.52%
CO	4242-4318	1170	240	0.46%	0.54%
O ₂	7765-8005	460	260	0.29%	0.37%

Table 3. The measurement precision of typical InGaAs spectra compared to InSb spectra for XCO₂ and XCO.

Detectors	Mean	Standard deviation	Precision
XCO ₂ _InGaAs	398.17ppm	0.17ppm	0.04%
XCO ₂ _InSb	397.15ppm	0.34ppm	0.09%
XCO_InGaAs	87.79ppb	0.94ppb	1.07%
XCO_InSb	94.85ppb	1.86ppb	2.00%



Table 4. Satellite data filtered criteria for GOSAT and OCO-2.

Variable (OCO-2 version 7Br)	Criteria
xco2_quality_flag	0
warn_level	≤ 12
Variable (OCO-2 version 7r)	Criteria
RetrievalResults/outcome_flag	1 or 2
RetrievalResults/xco2_uncert	< 1.5 ppm
PreprocessingResults/cloud_flag_abp	0
PreprocessingResults/cloud_flag_idp	2 or 3
PreprocessingResults/selection_priority	0
Variable (NIES-GOSAT)	Criteria
Data/retrievalQuality/totalPostScreeningResult	0
scanAttribute/qualityInformation/totalPreScreeningResult	0

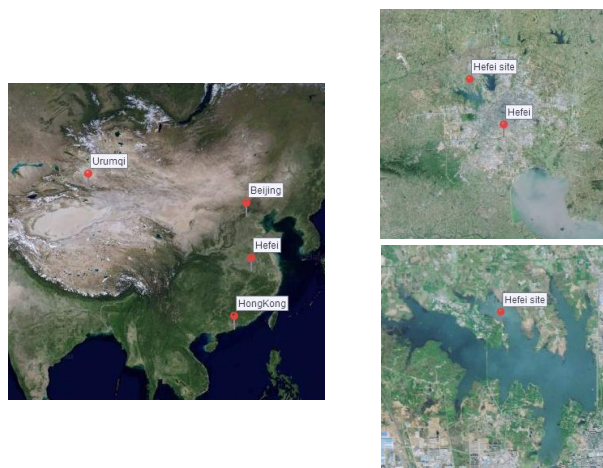


Figure 1. Map of China and location of Hefei site.



Figure 2. Bruker IFS 125HR spectrometer (left panel) and solar tracker (right panel).

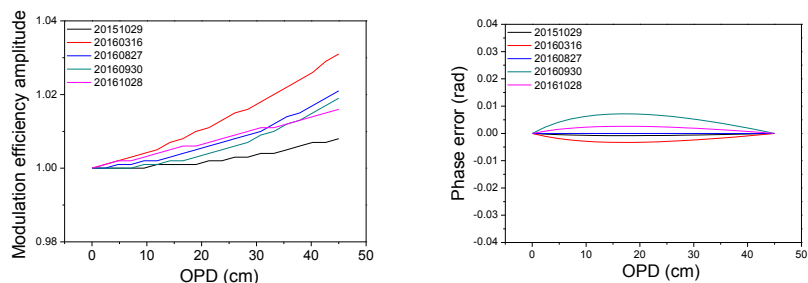


Figure 3. ME amplitudes (left panel) and phase errors (right panel) retrieved from HCl cell measurements.

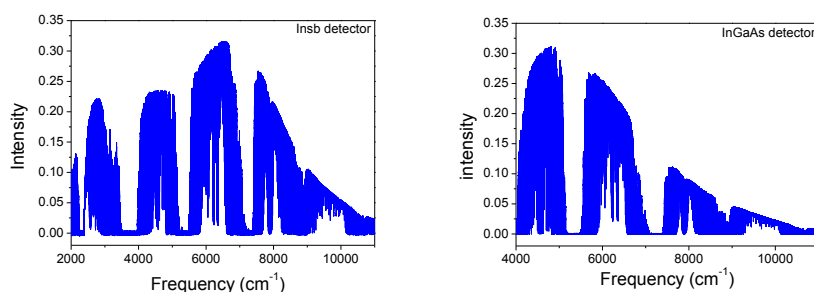


Figure 4. Typical solar spectra collected by InSb detector on October 24, 2014 (left panel) and InGaAs detector on August 4, 2015 (right panel), respectively.

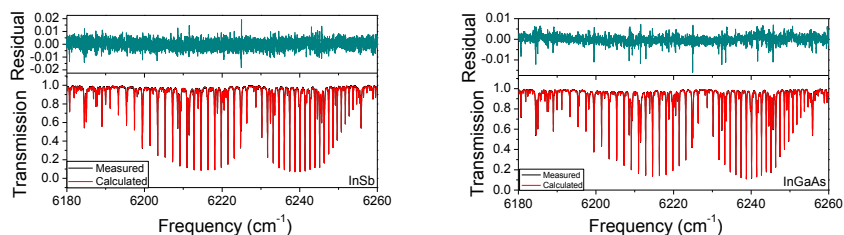


Figure 5. Spectral fitting of CO₂ in spectral window of 6180-6260cm⁻¹ using InSb detector (left panel) and InGaAs detector (right panel).

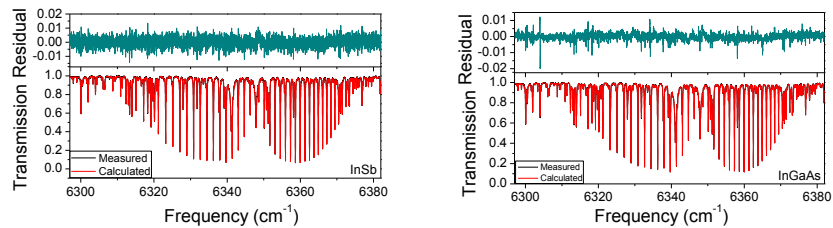


Figure 6. Spectral fitting of CO₂ in spectral window of 6297-6382cm⁻¹ using InSb detector (left panel) and InGaAs detector (right panel).

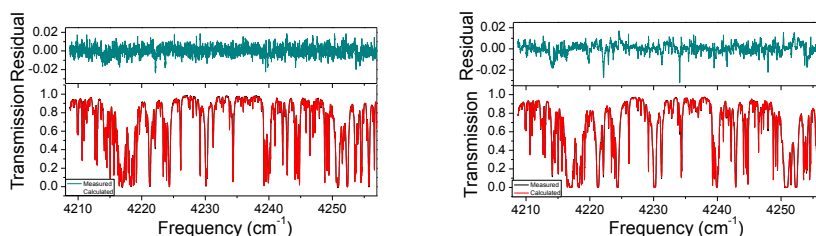


Figure 7. Spectral fitting of CO in spectral window of 4208-4257 cm^{-1} using InSb detector (left panel) and InGaAs detector (right panel).

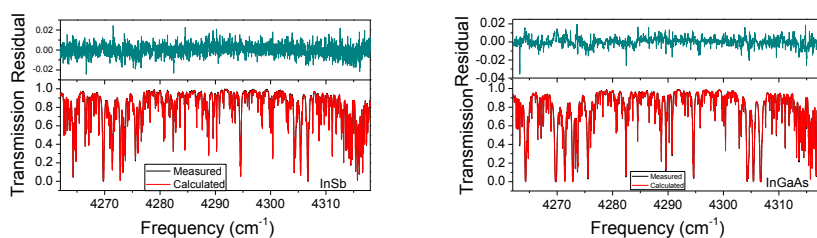


Figure 8. Spectral fitting of CO in spectral window of 4242-4318 cm^{-1} using InSb detector (left panel) and InGaAs detector (right panel).

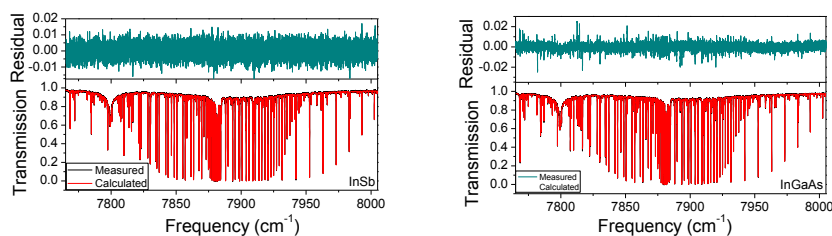


Figure 9. Spectral fitting of O_2 in spectral window of 7765-8005 cm^{-1} using InSb detector (left panel) and InGaAs detector (right panel).

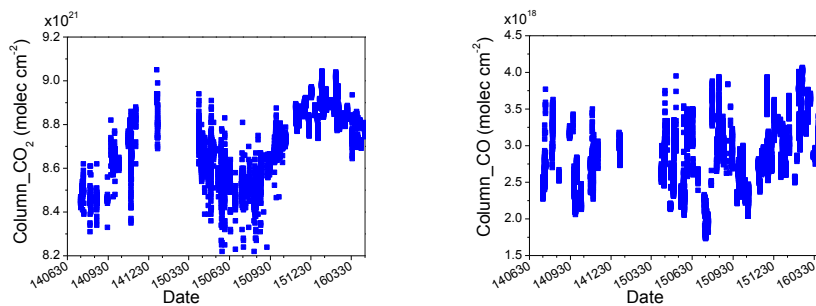


Figure 10. Time series of retrieved total column of CO_2 (left panel) and CO (right panel).

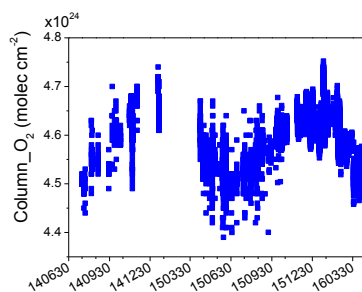


Figure 11. Time series of retrieved total column of O₂.

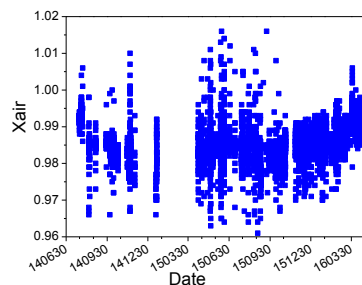


Figure 12. Time series of retrieved Xair.

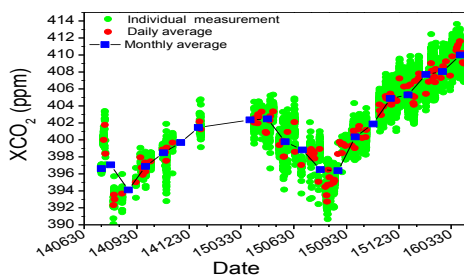


Figure 13. Time series of XCO₂ from July 2014 to April 2016 at Hefei. The green circles indicate individual XCO₂, the red circles represent daily averages of XCO₂, the black lines with blue squares represent monthly averages of XCO₂.

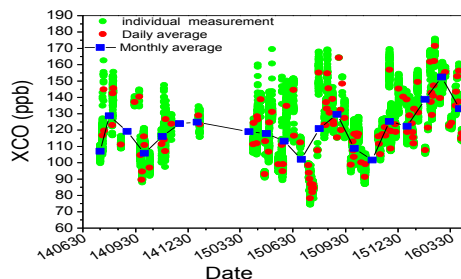


Figure 14. Time series of XCO from July 2014 to April 2016 at Hefei. The green circles indicate individual XCO, the red circles represent daily averages of XCO, the black lines with blue squares represent monthly averages of XCO.

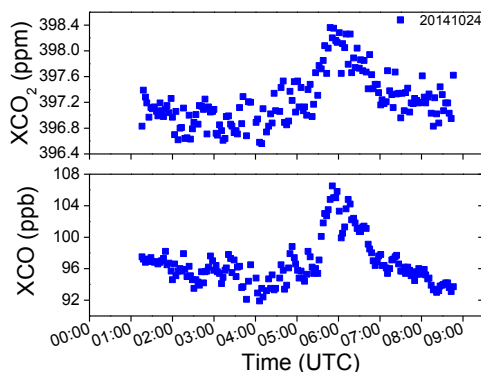


Figure 15. Time series of XCO₂ (top panel) and XCO (bottom panel) on October 24, 2014.

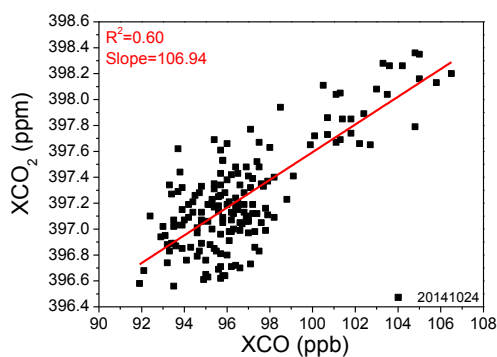


Figure 16. Correlation between XCO₂ and XCO on October 24, 2014.

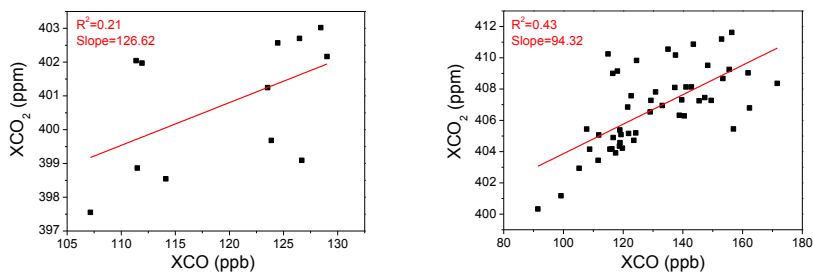


Figure 17. Correlation between XCO₂ and XCO in winter and spring for 2014-2015 (left panel) and 2015-2016 (right panel).

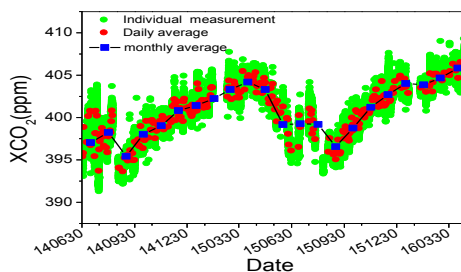


Figure 18. Time series of XCO₂ from July 2014 to April 2016 at Tsukua station. The green circles indicate individual XCO₂, the red circles represent daily averages of XCO₂, the black lines with blue circles represent monthly averages of XCO₂.

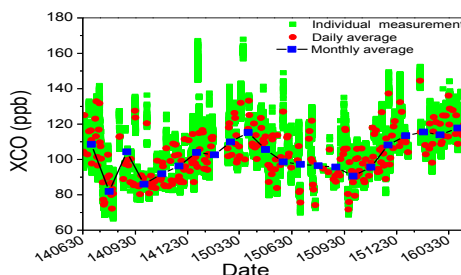


Figure 19. Time series of XCO from July 2014 to April 2016 at Tsukua station. The green circles indicate individual XCO, the red circles represent daily averages of XCO, the black lines with blue circles represent monthly averages of XCO.

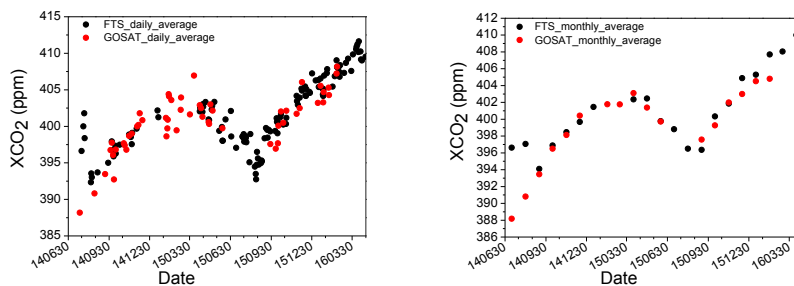


Figure 20. Comparison of ground-based observations with retrieved data from GOSAT, including daily averaged XCO₂ (left panel) and monthly averaged XCO₂ (right panel).

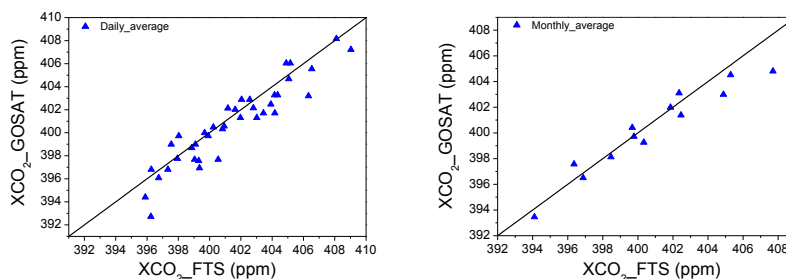


Figure 21. Scatter graph of daily averaged XCO₂ (left panel) and monthly averaged XCO₂ (right panel) for GOSAT and FTS.

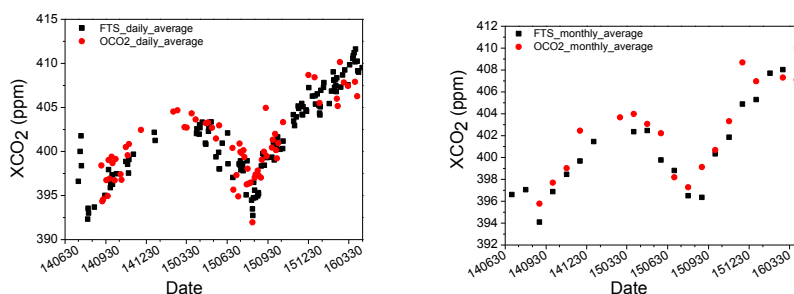


Figure 22. Comparison of ground-based observations with retrieved data from OCO2, including daily averaged XCO₂ (left panel) and monthly averaged XCO₂ (right panel).

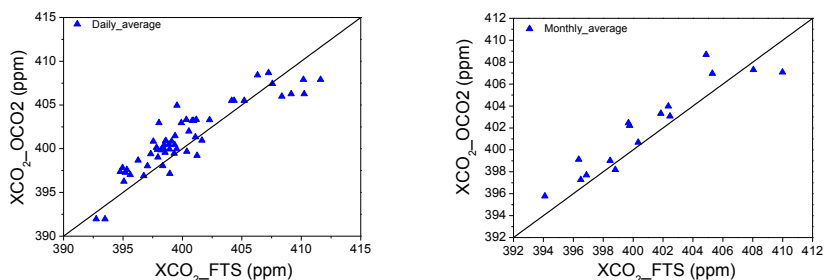


Figure 23. Scatter graph of daily (left panel) and monthly averaged XCO₂ (right panel) for OCO2 and FTS.